

PATH FOLLOWING OF STRAIGHT LINES AND CIRCLES FOR MARINE SURFACE VESSELS

Morten Breivik ^{*,1} Thor I. Fossen ^{*}

^{*} *Centre for Ships and Ocean Structures (CESOS), Norwegian University of Science and Technology (NTNU), NO-7491 Trondheim, Norway. E-mails: morten.breivik@ieee.org, tif@itk.ntnu.no*

Abstract: This paper addresses the problem of path following for marine surface vessels. A guidance-based approach which is equally applicable for land, sea and air vehicles is presented. The main idea is to explicitly control the velocity vector of the vehicles in such a way that they converge to and follow the desired geometrical paths in a natural and elegant manner. Specifically, straight lines and circles are considered. A nonlinear model-based controller is designed for a fully actuated vessel to enable it to comply with the guidance commands. The vessel is exposed to a constant environmental force, so integral action is added by means of parameter adaptation. A full nonlinear vessel model is used in the design. By introducing sideslip compensation and a dynamic controller state, the results are extended to underactuated vessels. *Copyright © 2004 IFAC*

Keywords: Marine surface vessels, Path following, Guidance, Line-of-Sight, Nonlinear model-based control, Underactuated vessels

1. INTRODUCTION

The ability to accurately maneuver a ship, a rig or a semi-submersible along a given path at sea is of primary importance for most applications. In this context, trajectory tracking systems for marine surface vessels are frequently proposed in the literature, see e.g. (Fossen 2002). Their task is to ensure that the vessel tracks a time-parametrized reference curve in the horizontal plane. However, there are weaknesses to the approach. Firstly, it does not take advantage of the geometric information about the desired path when it is available. It merely considers tracking an instantaneous, time-varying position signal. Hence, the way in which positional trajectory tracking is currently being performed is similar to ordinary servosystem tracking. This fact degrades the transient convergence behaviour of the position significantly, and makes it

unnatural. One solution to this weakness would be to design a guidance system which utilizes the available geometric information to ensure a natural convergence behaviour.

The second weakness can be illustrated by the following: suppose that a geometrically feasible trajectory is created for a vessel to negotiate. The trajectory is based on a prespecified speed assignment which the vessel must fulfil when tracking the path to satisfy certain time constraints. To ensure the design of a dynamically feasible time parametrization, information about the weather and the initial propulsion capability of the vessel is applied. But such features can change significantly during the voyage, resulting in a dynamically infeasible trajectory. The tracking point on the original trajectory will then leave the vessel behind, saturating the actuators and making the system unstable. A reparametrization can take care of this. However, it will have to consider the new situation, which also can change rapidly, to construct a feasi-

¹ Supported by the Norwegian Research Council through the Centre for Ships and Ocean Structures, Centre of Excellence at NTNU.

ble time parametrization given the current knowledge. This is not a smart or intuitive way to act. It does not correspond to the way in which we humans adapt dynamically to changing conditions when controlling vehicles. We do not aim at tracking a conceptual point in front of us if we understand that it would be equivalent with risking lives or damaging the vehicle. Hence, so should a trajectory reparametrization be dynamically adaptable. This can be done in the framework of path following, where the task objective is first and foremost to converge to the desired path, and secondly to satisfy a given dynamical assignment along the path. If the second objective cannot be satisfied, the vessel will still be able to follow the path, though not at the initial speed profile.

The main contribution of this paper is to remove the two principal weaknesses of the traditional trajectory tracking scheme. A guidance-based path following approach which ensures a natural maneuvering behaviour is presented. The guidance and control framework in which the approach is developed easily extends from fully actuated to underactuated vessels such that path following for the latter also is achieved. The considered geometrical paths are straight lines and circles.

2. PROBLEM STATEMENT

In path following, the primary objective concerning a vehicle is to restrict its position to a specific manifold represented by a desired geometric path. The secondary objective is to ensure that the vehicle complies with a desired dynamical behaviour while traversing the path. Consequently, the path following problem can be expressed by the following two task objectives:

Geometric Task: Make the position of the vessel converge to and follow a desired geometric path.

Dynamic Task: Make the speed of the vessel converge to and track a desired speed.

The next section is concerned with developing a guidance law which guarantees the fulfilment of the geometric task.

3. GUIDANCE SYSTEM DESIGN

The theory in this section is taken from (Breivik and Fossen 2004).

3.1 Guidance for a General Path

Consider a point mass particle situated on a two-dimensional surface. Denote the inertial position and velocity of the particle by $\mathbf{p} \in \mathbb{R}^2$ and $\mathbf{v} \in \mathbb{R}^2$, respectively. The velocity vector has two characteristics; size and orientation. Denote the size by $U = \|\mathbf{v}\|_2 = (\mathbf{v}^\top \mathbf{v})^{\frac{1}{2}}$ (the speed) and the orientation by $\chi = \arctan(\frac{v_y}{v_x})$ (the course angle). It is assumed that

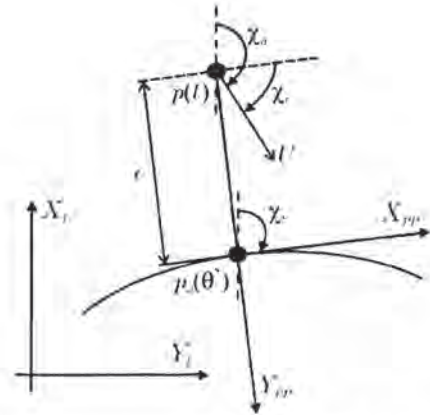


Fig. 1. A geometrical illustration of the guidance-based path following approach.

both U and χ can attain any desirable value instantaneously, consequently the point mass particle will be referred to as an ideal particle hereafter. Also defined on the two-dimensional surface is a geometrical path, parametrized by a scalar variable $\theta \in \mathbb{R}$. For any given θ , the inertial position of the geometrical path is denoted by $\mathbf{p}_d(\theta) \in \mathbb{R}^2$. Our main objective is to make the ideal particle converge to and live on this two-dimensional manifold.

Assume that a well-defined value of θ that minimizes the Euclidean distance between \mathbf{p} and $\mathbf{p}_d(\theta)$ exists. Denote this global minimizer θ^* and define it by:

$$\|\mathbf{p} - \mathbf{p}_d(\theta^*)\|_2 \triangleq \arg \min_{\theta \in \mathbb{R}} \|\mathbf{p} - \mathbf{p}_d(\theta)\|_2. \quad (1)$$

Define a local reference frame at $\mathbf{p}_d(\theta^*)$ and christen it the Path Parallel (PP) frame. The PP frame is rotated an angle:

$$\chi_t(\theta^*) = \arctan\left(\frac{y'_d(\theta^*)}{x'_d(\theta^*)}\right) \quad (2)$$

relative to the inertial frame, where the notation $x'_d(\theta) = \frac{dx_d}{d\theta}(\theta)$ has been used. Consequently, the x-axis of the PP frame is aligned with the tangential vector to the path at $\mathbf{p}_d(\theta^*)$.

The error vector between \mathbf{p} and $\mathbf{p}_d(\theta^*)$ expressed in the PP frame is:

$$\boldsymbol{\varepsilon} = \mathbf{R}_p^\top(\chi_t)(\mathbf{p} - \mathbf{p}_d(\theta^*)), \quad (3)$$

where:

$$\mathbf{R}_p(\chi_t) = \begin{bmatrix} \cos \chi_t & -\sin \chi_t \\ \sin \chi_t & \cos \chi_t \end{bmatrix} \quad (4)$$

is the rotation matrix from the inertial frame to the PP frame, $\mathbf{R}_p \in SO(2)$. By definition $\boldsymbol{\varepsilon} = [0, e]^\top$, where e is called the cross-track error to the path and represents the lateral distance to the path-tangent at $\mathbf{p}_d(\theta^*)$ as illustrated in Figure 1. The geometric task objective is achieved if $e \rightarrow 0$ as $t \rightarrow \infty$, which can be attained by developing a guidance law for the orientation of the velocity vector of the ideal particle.

We obtain the time-derivative of e by differentiating (3) with respect to time:

$$\dot{e} = U \sin(\chi - \chi_t), \quad (5)$$

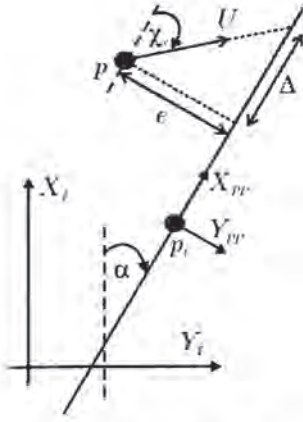


Fig. 2. LOS guidance for a straight line.

and since we are dealing with an ideal particle, we can assign the course angle of the velocity vector to a given desired course angle, i.e. $\chi = \chi_d$. Consequently, (5) can be rewritten as:

$$\dot{e} = U \sin(\chi_d - \chi_t), \quad (6)$$

where $(\chi_d - \chi_t)$ can be considered as a virtual input for stabilizing e . Denote this angular difference by $\chi_r = \chi_d - \chi_t$, i.e. the relative angle between the desired course and the path-tangential course. Obviously, such a variable should depend on e , such that $\chi_r = \chi_r(e)$. An attractive choice would be a physically motivated line-of-sight (LOS) angle like:

$$\chi_r(e) = \arctan\left(-\frac{e}{\Delta}\right), \quad (7)$$

where $\Delta > 0$ is a guidance parameter shaping the convergence to the path tangential. It is often referred to as the lookahead distance in literature treating path following of straight lines (Papoulias 1991). The physical interpretation of the LOS angle and the lookahead distance can be derived from Figure 2. Note that other shaping functions with arctan-like properties are possible candidates for $\chi_r(e)$, e.g. the tanh function.

When choosing $\chi_r(e)$ as in (7), the cross-track error dynamics becomes:

$$\begin{aligned} \dot{e} &= U \sin(\chi_r) \\ &= \frac{-Ue}{\sqrt{e^2 + \Delta^2}}, \end{aligned} \quad (8)$$

from which it can be derived that the origin of e is uniformly globally asymptotically and locally exponentially stable (UGAS/ULES) if the size of the velocity vector is required to be bounded from below, i.e. $U \geq U_{\min} > 0$. This serves as a theoretical justification for generally applying LOS guidance to obtain positional convergence.

To sum up, the desired course angle is given by:

$$\chi_d(\theta^*, e) = \chi_t(\theta^*) + \chi_r(e), \quad (9)$$

with $\chi_t(\theta^*)$ as in (2) and $\chi_r(e)$ as in (7).

By stabilizing the origin of e , the path following geometric task is achieved. The dynamic task is satisfied

by making sure that $U = \dot{U}_d \geq U_{d,\min} > 0$, which is a control problem and not a guidance problem. The subject of finding the global minimizer θ^* that gives e for a general geometrical path is not treated in this paper. Since e can easily be computed directly for straight lines and circles such geometrical topologies are considered.

3.2 Guidance for a Straight Line

Denote an arbitrary point on a straight line as $p_l \in \mathbb{R}^2$. The line is rotated an angle α and defined relative to the origin of a local reference frame in \mathbb{R}^2 . The cross-track error can easily be calculated by extracting the second element of:

$$e = R_p^T(\alpha)(p - p_l), \quad (10)$$

from which we can calculate χ_d as:

$$\chi_d(e) = \chi_t + \chi_r(e) = \alpha + \chi_r(e), \quad (11)$$

where $\chi_r(e)$ is given by (7). See Figure 2 for an illustration of this.

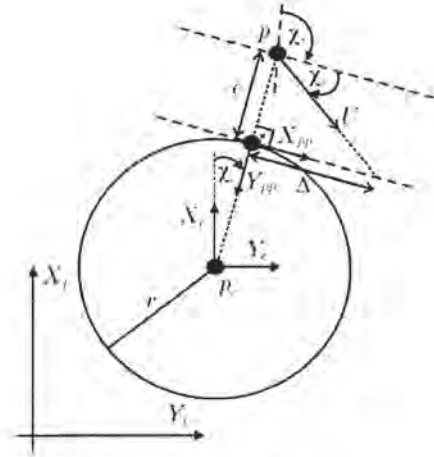


Fig. 3. LOS guidance for a circle.

3.3 Guidance for a Circle

Denote the centre of a circle as $p_c \in \mathbb{R}^2$. The circle is defined relative to the origin of a local reference frame in \mathbb{R}^2 . Contrary to a straight line, a circle has non-zero curvature. Consequently, χ_t changes with time. By inspection of Figure 3, this angle can easily be deduced as either:

$$\chi_t(t) = \chi_c(t) + \frac{\pi}{2} \quad (12)$$

or:

$$\chi_t(t) = \chi_c(t) - \frac{\pi}{2}, \quad (13)$$

where:

$$\chi_c(t) = \arctan\left(\frac{y(t) - y_c}{x(t) - x_c}\right). \quad (14)$$

Equation (12) gives a clockwise circular motion, whilst (13) represents an anti-clockwise motion.

Denote the radius of the circle as $r \in \mathbb{R}_+$. The cross-track error can then be computed by:

$$e(t) = r - \|\mathbf{p}(t) - \mathbf{p}_c\|_2, \quad (15)$$

as derived from Figure 3. The desired course angle χ_d is calculated by feeding e into equation (7) and summing the result with (12) or (13).

4. DEFINITIONS OF COURSE, HEADING AND SIDESLIP ANGLES

The relationship between the angular variables *course*, *heading* and *sideslip* is important for maneuvering a marine surface vessel. The terms course and heading are used interchangeably in most of the literature on control of marine vessels. Consequently, definitions utilizing a consistent symbolic notation should be established and enforced. The relationship between the angular variables is illustrated in Figure 4, and defined below. In this context, the NED frame is a local geographic reference frame, while the BODY frame is the vessel-fixed reference frame, both as defined in (Fossen 2002).

Definition 1. *Course angle* χ : The angle from the x-axis of the NED frame to the velocity vector of the vessel, positive rotation about the z-axis of the NED frame by the right-hand screw convention.

Definition 2. *Heading (yaw) angle* ψ : The angle from the x-axis of the NED frame to the x-axis of the BODY frame, positive rotation about the z-axis of the NED frame by the right-hand screw convention.

Definition 3. *Sideslip (drift) angle* β : The angle from the x-axis of the BODY frame to the velocity vector of the vessel, positive rotation about the z-axis of the BODY frame by the right-hand screw convention.

By these definitions, it is apparent that

$$\chi = \psi + \beta, \quad (16)$$

where:

$$\beta = \arcsin\left(\frac{v}{U}\right) \xrightarrow{\beta \text{ small}} \beta \approx \frac{v}{U}, \quad (17)$$

which is easily verified from Figure 4.

Remark 4. (The Society of Naval Architects and Marine Engineers 1950) defines the sideslip angle for marine vessels according to

$$\beta_{SNAME} = -\beta,$$

which can also be found in (Lewis, E.V. (Ed.) 1989). However, the sign convention chosen here follows that of the aircraft community, see e.g. (Nelson 1998) and (Stevens and Lewis 2003), which is more convenient from a guidance point-of-view.

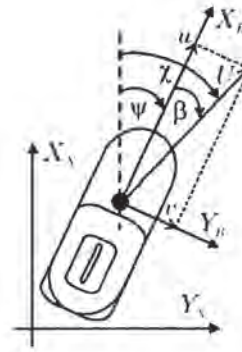


Fig. 4. The geometrical relationship $\chi = \psi + \beta$ between the course (χ), heading (ψ) and sideslip (β) angles.

The heading angle equals the course angle ($\psi = \chi$) when the sway velocity is zero ($v = 0$), i.e. when there is no sideslip. This is generally attainable for fully actuated vessels, but not for those which are unactuated in the sway direction, which affects the design of guidance systems for such vessels. Specifically, to achieve path following for these vessels, the heading angle must be actively used to direct the velocity vector in the desired direction by using so-called sideslip compensation. This means that the desired heading angle must be computed by $\psi_d = \chi_d - \beta$.

5. CONTROL SYSTEM DESIGN

It is usually sufficient to consider only the 3 horizontal degrees-of-freedom (DOF) when designing control systems for marine surface vessels. The 3 DOF kinematics and dynamics can be represented as (Fossen 2002):

$$\dot{\eta} = \mathbf{R}(\psi)\boldsymbol{\nu} \quad (18)$$

and:

$$\mathbf{M}\dot{\boldsymbol{\nu}} + \mathbf{C}(\boldsymbol{\nu})\boldsymbol{\nu} + \mathbf{D}(\boldsymbol{\nu})\boldsymbol{\nu} = \boldsymbol{\tau} + \mathbf{R}(\psi)^T \mathbf{b}, \quad (19)$$

where $\eta = [x, y, \psi]^T \in \mathbb{R}^3$ represents the earth-fixed position and heading, $\boldsymbol{\nu} = [u, v, r]^T \in \mathbb{R}^3$ represents the vessel-fixed velocities, $\mathbf{R}(\psi) \in SO(3)$ is the rotation matrix from the earth-fixed local geographic reference frame (NED) to the vessel-fixed reference frame (BODY), \mathbf{M} is the vessel inertia matrix, $\mathbf{C}(\boldsymbol{\nu})$ is the centrifugal and coriolis matrix, $\mathbf{D}(\boldsymbol{\nu})$ is the hydrodynamic damping matrix, $\boldsymbol{\tau}$ represents the vessel-fixed propulsion forces and moments, and \mathbf{b} describes the earth-fixed LF environmental forces acting on the vessel. The system matrices in (19) are assumed to satisfy the properties $\mathbf{M} = \mathbf{M}^T > 0$, $\mathbf{C} = -\mathbf{C}^T$ and $\mathbf{D} > 0$. It is further assumed that the vessel has port-starboard symmetry. This is highly valid for most cases, whereas an additional assumption of fore-aft symmetry (Pettersen and Lefeber 2001) is far more questionable because it implies uncoupled sway and yaw dynamics.

A fully actuated vehicle is able to command independent accelerations in all relevant DOFs simulta-

neously. Consequently, the control vector for a fully actuated marine surface vessel is given by:

$$\tau = [\tau_1, \tau_2, \tau_3]^T, \quad (20)$$

where τ_1 represents the force input in surge, τ_2 represents the force input in sway and τ_3 represents the moment input in yaw.

The control law design is performed in two steps by using the backstepping technique for nonlinear systems (Krstić *et al.* 1995), and is an extension of the work in (Fossen *et al.* 2003). Specifically, environmental disturbances and a more complex vessel model is considered. Care is also taken to avoid compensating for valuable hydrodynamical damping terms. The main results of the controller design are stated in what follows.

The projection vector \mathbf{h} is defined by:

$$\mathbf{h}^T \triangleq [0, 0, 1], \quad (21)$$

while the error variables $z_1 \in \mathbb{R}$ and $\mathbf{z}_2 \in \mathbb{R}^3$ are defined by:

$$z_1 \triangleq \psi - \psi_d = \mathbf{h}^T \boldsymbol{\eta} - \psi_d \quad (22)$$

$$\mathbf{z}_2 \triangleq [z_{2,1}, z_{2,2}, z_{2,3}]^T = \boldsymbol{\nu} - \boldsymbol{\alpha}, \quad (23)$$

where $\boldsymbol{\alpha} = [\alpha_1, \alpha_2, \alpha_3]^T \in \mathbb{R}^3$ is a vector of stabilizing functions to be defined later.

The following Control Lyapunov Function (CLF) is considered:

$$V = \frac{1}{2} z_1^2 + \frac{1}{2} \mathbf{z}_2^T \mathbf{M} \mathbf{z}_2 + \frac{1}{2} \tilde{\mathbf{b}}^T \boldsymbol{\Gamma}^{-1} \tilde{\mathbf{b}} > 0, \quad (24)$$

where $\tilde{\mathbf{b}}$ is an adaptation error defined as $\tilde{\mathbf{b}} \triangleq \mathbf{b} - \hat{\mathbf{b}}$ with $\hat{\mathbf{b}}$ being the estimate of \mathbf{b} . By assumption, $\dot{\mathbf{b}} = 0$. $\boldsymbol{\Gamma} = \boldsymbol{\Gamma}^T > 0$ is the adaptation gain matrix.

By choosing the control input as:

$$\tau = \mathbf{M} \dot{\boldsymbol{\alpha}} + \mathbf{C} \boldsymbol{\alpha} + \mathbf{D} \boldsymbol{\alpha} - \mathbf{R}^T \hat{\mathbf{b}} - \mathbf{h} z_1 - \mathbf{K}_2 \mathbf{z}_2 \quad (25)$$

and the parameter adaptation as:

$$\dot{\hat{\mathbf{b}}} = \boldsymbol{\Gamma} \mathbf{R} \mathbf{z}_2 \quad (26)$$

we finally obtain:

$$\dot{V} = -k_1 z_1^2 - \mathbf{z}_2^T (\mathbf{D} + \mathbf{K}_2) \mathbf{z}_2 \leq 0, \quad (27)$$

where $k_1 > 0$, $\mathbf{K}_2 = \text{diag}(k_{2,1}, k_{2,2}, k_{2,3}) > 0$ and $\boldsymbol{\alpha} = [u_d, 0, -k_1 z_1 + \dot{\psi}_d]^T$. Notice that the inherent damping properties of the system have been preserved.

The main result of the control design is summarized by the following proposition:

Proposition 5. For smooth reference trajectories ψ_d , $\dot{\psi}_d$ and $\ddot{\psi}_d \in \mathcal{L}_\infty$ and $u_d, \dot{u}_d \in \mathcal{L}_\infty$, the origin of the error system $(z_1, \mathbf{z}_2, \tilde{\mathbf{b}})$ becomes uniformly globally asymptotically and locally exponentially stable (UGAS/ULES) by choosing the control and disturbance adaptation laws as in (25) and (26), respectively.

PROOF. [Sketch] By collecting the error states in the vector $\mathbf{z} = [z_1, \mathbf{z}_2^T]^T$ and rewriting their dynamics in a manner which is motivated by Theorem A.5 in (Fossen 2002), UGAS/ULES of the origin of the error system can easily be proven.

An underactuated vehicle has fewer independent control inputs available simultaneously than there are number of DOFs to be controlled. Specifically, we consider underactuation in the sway direction:

$$\tau = [\tau_1, 0, \tau_3]^T, \quad (28)$$

which represents the most common actuator configuration among vessels travelling at high speeds.

Since τ_2 is not available to implement the required terms for the sway direction, dynamics can be imposed on the corresponding stabilizing function such that (25) is still satisfied (Fossen *et al.* 2003). In our particular case, an analysis of the α_2 -subsystem reveals that the sway speed of the underactuated vessel remains bounded. An analysis of what happens to v is seldom performed for underactuated vessels. Traditionally, this is true for literature treating autopilot design by the Nomoto model (Fossen 2002), but even nonlinear control design concepts disregard the analysis (Lapierre *et al.* 2003).

Sway-underactuated vessels is extensively treated in the literature. Most approaches only consider diagonal system matrices and no environmental disturbances. However, (Do and Pan 2003) lifts these assumptions. Unfortunately, exact path following for an arbitrary point cannot be achieved by this approach since it requires the controlled point to be located where the system matrices become diagonal. Also, u is required to exceed v . Such restrictions are not imposed in this paper.

6. CASE STUDY: AN UNDERACTUATED MARINE SURFACE VESSEL

To illustrate the performance of the proposed guidance and control scheme, a simulation is performed with an underactuated marine surface vessel trying to follow a straight line path while being exposed to a constant environmental force. The vessel data is taken from the model ship Cybership 2, a 1:70 scale model of a supply vessel, which has a mass of $m = 23.8 \text{ kg}$ and a length of $L = 1.255 \text{ m}$. See (Skjetne 2004) for the exact model parameters. The vessel is considered to be unactuated in the sway direction, as in (28).

The desired path is a straight line with $\alpha = \frac{\pi}{4}$. It runs through the origin of the NED frame. The environmental disturbance acts perpendicular to the path with a size of about 2.10 N . Specifically, $\mathbf{b} = [-1.5 \text{ (N)}, 1.5 \text{ (N)}, 0 \text{ (Nm)}]^T$. The initial states are chosen to be $\boldsymbol{\eta}_0 = [10 \text{ (m)}, 0 \text{ (m)}, 1.3 \text{ (rad)}]^T$ and $\boldsymbol{\nu}_0 = [0.25 \text{ (m/s)}, 0 \text{ (m/s)}, 0 \text{ (rad/s)}]^T$, where the

initial surge speed is to be kept during the run. The controller gains are chosen as $k_1 = 10$, $k_{2,1} = 10$, $k_{2,2} = 1$ and $k_{2,3} = 10$, while $\Gamma = \mathbf{I}$. The LOS guidance parameter is chosen to be $\Delta = 5L$.

Figure 5 shows that the vessel converges nicely to the path, which would have been impossible without sideslip compensation. Figure 6 illustrates that the cross-track error converges exponentially to zero.

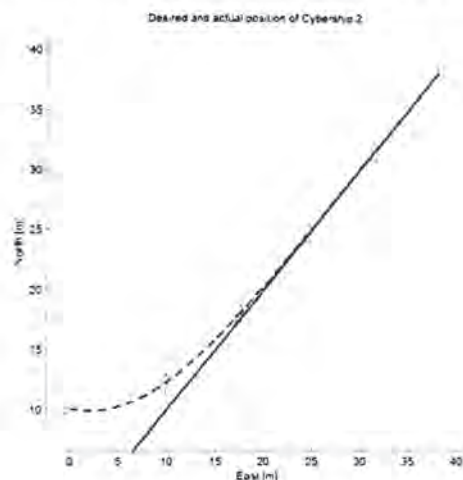


Fig. 5. Cybership 2 converges naturally to the desired path.

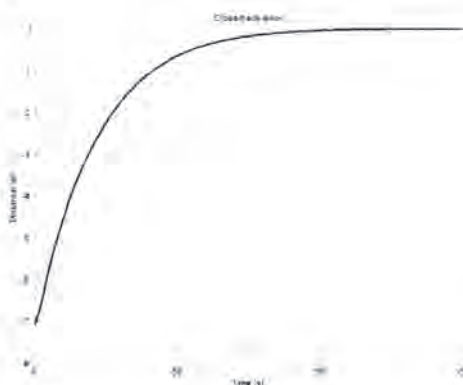


Fig. 6. The cross-track error converges exponentially to zero.

7. CONCLUSION

This paper has presented a guidance-based path following approach to maneuvering marine surface vessels. The approach is equally applicable for land, sea and air vehicles and eliminates the two main weaknesses associated with a traditional trajectory tracking scheme. Specifically, a line-of-sight implementation of the approach has been used to illustrate the following of straight lines and circles. The total contribution is a guidance and control scheme which fulfils the path following objective for both fully actuated and underactuated vessels. Simulation results quantitatively confirm the successful performance of the guidance and control strategy. The paper also contains

unambiguous definitions of the variables course, heading and sideslip as an attempt to avoid further confusion on the subject. Finally, it should be emphasized that the guidance scheme with sideslip compensation probably could improve the path following behaviour of existing vessels equipped with standard industrial autopilots. In most cases this would only require a software fix to the existing guidance system, which is highly financially viable. This adds an immediate practical flavour to the results.

REFERENCES

- Breivik, M. and T.I. Fossen (2004). Guidance for path following and trajectory tracking. *Journal of Guidance, Control, and Dynamics*. To be submitted.
- Do, K.D. and J. Pan (2003). Global tracking control of underactuated ships with off-diagonal terms. In: *Proceedings of the 42nd IEEE CDC, Maui, Hawaii, USA*.
- Fossen, T.I. (2002). *Marine Control Systems: Guidance, Navigation and Control of Ships, Rigs and Underwater Vehicles*. 1st ed.. Marine Cybernetics.
- Fossen, T.I., M. Breivik and R. Skjetne (2003). Line-of-sight path following of underactuated marine craft. In: *Proceedings of the 6th IFAC MCMC, Girona, Spain*.
- Krstić, M., I. Kanellakopoulos and P.V. Kokotović (1995). *Nonlinear and Adaptive Control Design*. John Wiley & Sons Inc.
- Lapierre, L., D. Soetanto and A. Pascoal (2003). Nonlinear path following with applications to the control of autonomous underwater vehicles. In: *Proceedings of the 42nd IEEE CDC, Maui, Hawaii, USA*.
- Lewis, E.V. (Ed.) (1989). *Principles of Naval Architecture*. Vol. III. The Society of Naval Architects and Marine Engineers.
- Nelson, R.C. (1998). *Flight Stability and Automatic Control*. 2nd ed.. McGraw-Hill.
- Papoulias, F.A. (1991). Bifurcation analysis of line of sight vehicle guidance using sliding modes. *International Journal of Bifurcation and Chaos* 1(4), 849–865.
- Pettersen, K.Y. and E. Lefeber (2001). Way-point tracking control of ships. In: *Proceedings of the 40th IEEE CDC, Orlando, Florida, USA*.
- Skjetne, R. (2004). A nonlinear ship manoeuvring model: Identification and adaptive control with experiments for a model ship. *Modeling, Identification and Control* 25(1), 3–27.
- Stevens, B.L. and F.L. Lewis (2003). *Aircraft Control and Simulation*. 2nd ed.. John Wiley & Sons Inc.
- The Society of Naval Architects and Marine Engineers (1950). Nomenclature for treating the motion of a submerged body through a fluid. Technical and Research Bulletin No. 1-5.